# High Isolated X-Band MIMO Array Using Novel Wheel-Like Metamaterial Decoupling Structure

**Jianfeng Jiang [1], Yinfeng Xia [1], and Yingsong Li [1,2,*]**

[1] College of Information and Communication Engineering
Harbin Engineering University, Harbin 150001, China

[2] Key Laboratory of Microwave Remote Sensing, National Space Science Center
Chinese Academy of Sciences, Beijing 100190, China
*liyingsong@ieee.org

***Abstract*** ─ A compact broadband antenna array with two identical antenna elements is proposed to realize high isolation that is realized via integrating a new wheel-like meta-material structure into the closely set antenna elements. The wheel-like meta-material decoupling structure is settled between the two antenna elements to reduce the coupling from the nearby antenna element. The proposed antenna array is designed, optimized, fabricated and measured in a chamber. The achieved results verify that the developed antenna is able to provide a wide bandwidth ranging from 8 GHz to 12 GHz. Using the developed wheel-like meta-material decoupling structure, not only the designed antenna array maintains performance of MIMO array, but also the coupling is reduced to be less than -20 dB within the X-band. Therefore, the proposed antenna array is a suitable candidate for X-band MIMO radar system applications to get a high isolation between the elements.

***Index Terms*** ─ High isolation, low mutual coupling, meta-material, MIMO antenna, wideband.

## I. INTRODUCTION

With the rapid evolution of the wireless communications and radar technology, the bandwidth requirements for these systems become to be wider and wider to obtain high data speed and resolution [1,2]. Thus, the wideband technology has been paid lots of attentions and gotten significant evolutions [3,4]. However, in wideband systems, reflection and diffraction can cause multipath fading problems, and hence, many researchers have moved to study MIMO technology to find out solutions for these problems. On the other hand, the MIMO technology can also improve the channel capacity and system reliability [5-7]. As a result, the combination of broadband technology and MIMO technology has drawn great concern in recent years.

In fact, with the increasing number of the antennas in the MIMO system, the distance between the antenna elements becomes to be narrow in the miniaturized devices, resulting in serious coupling affect from neighbored antenna elements [8-9]. To maintain the independence of each antenna elements in the MIMO system within a limited space, it is one of the urgent difficulties to overcome mutual coupling from the adjacent antenna elements. Therefore, the many recent research works are mainly focused on designing miniaturized MIMO antenna array integrating with decoupling structure.

In order to implement a high isolation MIMO antenna array, the defected ground structure (DGS) can change the current path on the ground plane to equal the combination of inductance and capacitance, modifying the electric field distribution between the transmission line and the ground plane to achieve the purpose of decoupling [10-12]. Also, the neutralization lines and other decoupling network have been presented to achieve the good isolation by introducing counter phased current against the excited antenna in development of the MIMO antenna array [13-16]. Recently, the meta-material structures have been considered to reduce the isolation between the adjacent antenna elements. The meta-material is a class of artificial composite structural material that can respond to external electromagnetic fields, which includes left-hand material, Electromagnetic Band Gap (EBG) structure, the Frequency Selective Surface (FSS) and so on. In [17-20], EBG structure have been proposed to reduce the mutual coupling using the suppression of surface waves. In [21-23], the FSS is suspended over the antenna array to increase isolation performance. However, these meta-materials cannot cover a wide bandwidth for X-band communication applications.

In this article, a compact wideband MIMO antenna with a novel wheel-like meta-material structure is presented and analyzed numerically and experimentally. The designed MIMO antenna array is made up of

*Submitted On: August 17, 2019*
*Accepted On: October 23, 2019*

two identical rectangular patch antennas on the same substrate, and the proposed wheel-like meta-material structure, which has three cells, is inserted into the middle of the antenna elements. The proposed MIMO antenna array is created, modeled, optimized, fabricated and measured to verify the effectiveness of the proposed MIMO array. The results show that the proposed MIMO antenna array can cover the frequency band of 8 GHz and 12 GHz, with omnidirectional radiation patterns and high isolation of 20 dB.

This paper is organized as follows: in Section II, the configuration of the MIMO antenna array and meta-material structure are proposed. Section III analyzes and discusses the simulated and measured results of the developed MIMO antenna array. Finally, a conclusion is given in Section IV.

## II. DESIGN OF THE PROPOSED WIDEBAND MIMO ANTENNA ARRAY

### A. The proposed MIMO antenna array structure

The configuration of the proposed MIMO antenna array is modeled in HFSS 13.0 and is shown in Fig. 1. As shown in Fig. 1, the dimensions of antenna array are $26 \times 18 \times 1.6$ mm$^3$, and the two patch antenna elements are printed on a substrate with permittivity of 4.4, a loss tangent of 0.02 and a thickness of h=1.6 mm. The proposed antenna is fed by microstrip line with a width of 3 mm.

In order to obtain wide bandwidth, a stub is integrated with the ground plane. Fig. 2 shows that the stub can increase the bandwidth. Furthermore, there are two small gaps in each patch antenna element to obtain the good matching by controlling the width and length of gaps.

Finally, the proposed MIMO antenna array is optimized using the HFSS to let the MIMO array operate at the X-band, and the optimized dimension of the MIMO array is listed in Table 1.

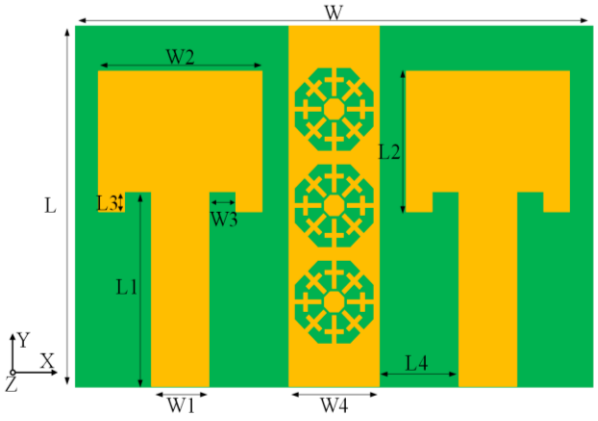


(a) Top view

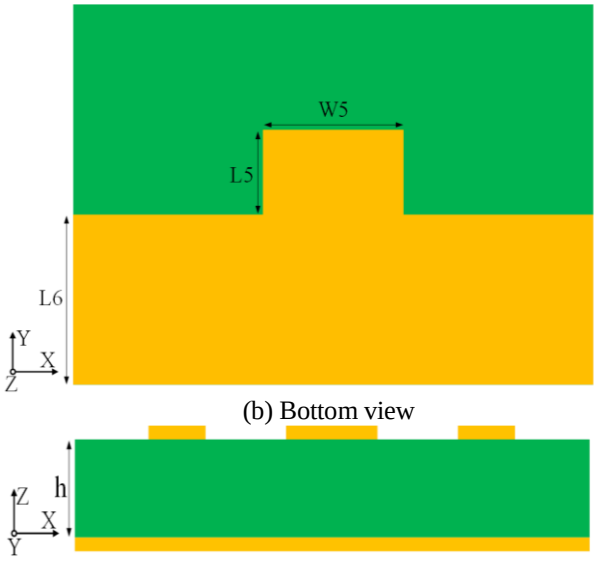


(b) Bottom view

(c) Side view

Fig. 1. Geometry structure of the proposed MIMO antenna array integrating with wheel-like meta-material structure.

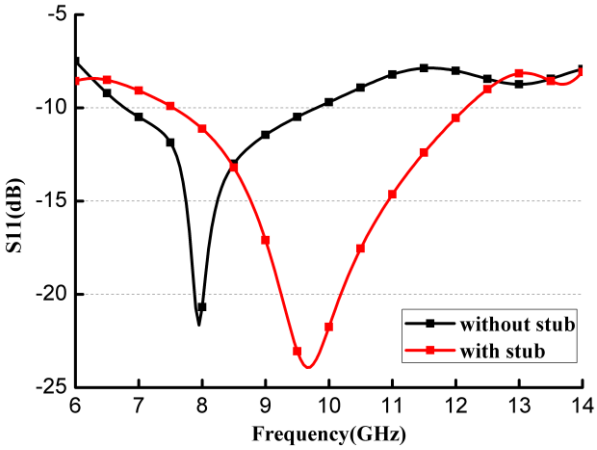


Fig. 2. $S_{11}$ of the wideband MIMO antenna array with and without stub.

Table 1: Optimized dimensions of the MIMO antenna array (Unit: mm)

| Parameters | W | W1 | W2 | W3 | W4 |
|---|---|---|---|---|---|
| Values | 26 | 3 | 8.5 | 1.4 | 4.5 |
| Parameters | W5 | L | L1 | L2 | L3 |
| Values | 7 | 18 | 9.7 | 7 | 1 |
| Parameters | L4 | L5 | L6 | h | |
| Values | 4.25 | 4 | 8 | 1.6 | |

### B. Meta-material decoupling structure

In Fig. 1, there is a wheel-like meta-material

structure between the proposed antenna elements. However, there is still having surface wave interferences that will affect the performance of the other antenna elements. If the influences of surface waves can be reduced, the characteristics of the MIMO antenna array will be improved. One effective method is to increase the distance between the two antennas, but this method does not meet the trend of miniaturization of electronic devices and is limited by the space in the portable devices. On the other hand, adding a decoupling network in the MIMO antenna array to suppress the propagation of surface waves has attracted much more attention in recent years. As we know, the meta-material structure has the property of suppressing surface waves, and hence, it can be used in the MIMO antenna array to reduce the mutual coupling between the MIMO antenna elements and can maintain good performance with closely antenna elements.

A meta-material decoupling cell used in the proposed MIMO antenna array is shown in Fig. 3, which is comprised of a copper patch with an octagon slot, eight crosses and a small octagon patch in the center. The diagonal length (W7) of the largest octagon slot is 4.5 mm and the diagonal length (W8) of the small octagon is 1.1 mm. The eight identical crosses are connected to the sides of the octagonal slot, the width (v) of the crosses is 0.2 mm. In addition, the length (L9) of the crosses is 1.4 mm, and the width (W9) of the crosses is 0.95 mm.

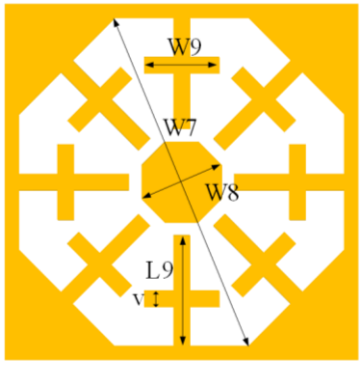


Fig. 3. Geometry structure of the proposed wheel-like meta-material cell.

In order to better validate the effectiveness of the proposed wheel-like meta-material cell, the meta-material cell is investigated by HFSS, and its effective parameters, such as equivalent permittivity $\varepsilon$ and equivalent permeability $\mu$, can be calculated from S-parameters [24], which is presented in formula (1) - (4):

$$z = \pm\sqrt{\frac{(1+S_{11})^2 - S_{21}^2}{(1-S_{11})^2 - S_{21}^2}}, \tag{1}$$

$$e^{jnkd} = \frac{S_{21}}{1 - S_{11}\dfrac{z-1}{z+1}}, \tag{2}$$

$$\varepsilon = \frac{n}{z}, \tag{3}$$

$$\mu = n \cdot z, \tag{4}$$

where $k$ is the wave number in free space, $d$ is the thickness of the meta-material structure cell, $n$ is the refractive index, $z$ is the wave impedance, $\varepsilon$ is the equivalent permittivity, and $\mu$ is the equivalent permeability.

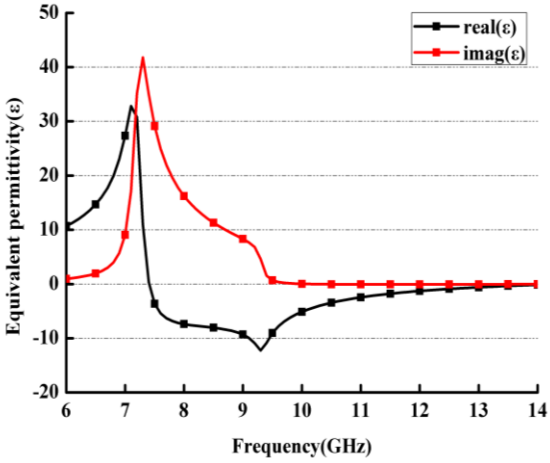


(a) Equivalent permittivity

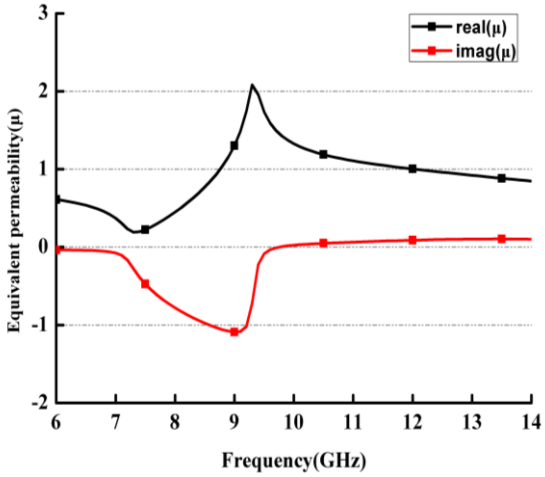


(b) Equivalent permeability

Fig. 4. Equivalent permittivity and permeability of the proposed meta-material cell.

Therefore, the equivalent permittivity and permeability of the meta-material cell can be calculated and shown in Fig. 4. It is noticed that the designed cell has a negative permittivity and positive permeability in entire X-band, which means that the designed meta-

material cell can meet the meta-material properties. According to the equation (5),

$$k^2 = \omega^2 \mu\varepsilon , \quad (5)$$

which is the dispersive equation of plane electromagnetic waves, it can be concluded that $k$ has no solution, result in suppressing the propagation of surface waves and achieving the purpose of decoupling. Thus, the proposed meta-material structure can be suitable for improve the isolation of X-band MIMIO antenna array.

## III. ANALYSISES RESULTS

The proposed wideband MIMO antenna array is constructed and analyzed based on the HFSS 13.0. To further verify the analysis effectiveness, the proposed antenna array is fabricated and presented in Fig. 5. The measured results were obtained using vector network analyzer (VNA) E5063A.

The simulation and measurement S-parameters including the reflection coefficient ($S_{11}$) and transmission coefficient ($S_{12}$) are shown in Fig. 6. It is noted that the proposed wideband MIMO antenna array without the proposed wheel-like meta-material decoupling structure has a bandwidth ranging from 8 GHz to 12 GHz. By using the proposed wheel-like meta-material decoupling structure, the bandwidth of the proposed MIMO antenna array moves to 7 GHz-12 GHz. That is to say that the operating frequency band moves to low frequency, and there is another resonance mode is appeared because of the resonance of the proposed wheel-like meta-material decoupling structure. It is noticed that mutual coupling that is measured using $S_{12}$ is reduce from -13 dB to less than -20 dB in the operating band of the proposed MIMO antenna array. The MIMO antenna can cover the X-band if we consider $S_{11}$ is less than -10 dB. It is also found that the resonance frequency is 9.7 GHz for the MIMO antenna array without the wheel-like meta-material decoupling structure, while there are two resonance frequencies locating at 9.7 GHz and 10.35 GHz, respectively.

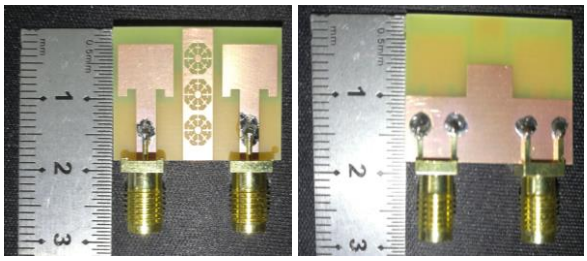

(a) Top view (b) Bottom view

Fig. 5. Photograph of the fabricated broadband MIMO antenna.

Figure 6 (b) depicts the comparison of the simulation and measurement of the S-parameters for proposed MIMO antenna array with the wheel-like meta-material decoupling structure. In the X-Band, $S_{11}$ is still less than -10 dB from the measurement, while the $S_{12}$ is less than -20 dB. It is found that the two resonance frequencies are shifted to the high frequency, which may be caused by the inaccuracy of the dimensions of the fabrication. However, the simulated and the measured results meet well in the operating band, which tells us that the proposed wheel-like meta-material decoupling structure can effectively reduce the mutual coupling between the antenna elements and maintains the bandwidth of the MIMO antenna array.

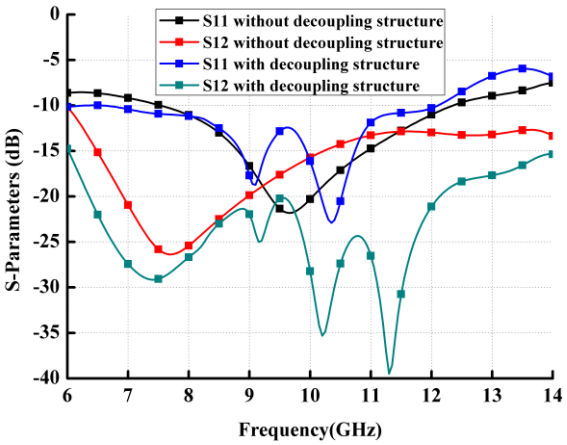


(a) With/without the proposed wheel-like meta-material decoupling structure

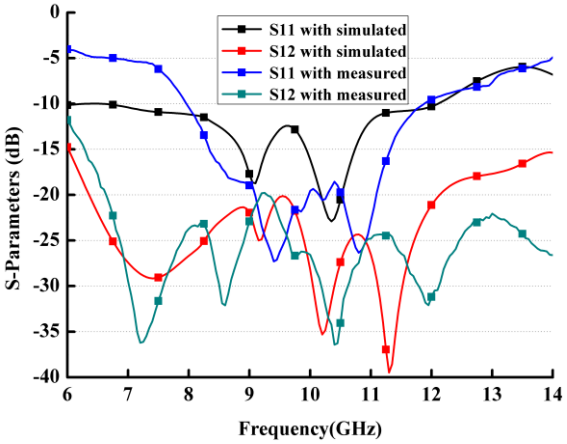


(b) Simulated and measured S-parameters of the proposed MIMO antenna array

Fig. 6. $S_{11}$ and $S_{12}$ of the wideband MIMO antenna array.

Figure 7 shows the xoz-plane and yoz-plane radiation patterns of the designed MIMO antenna array with comparison of the simulated and measured results. In the measurement, one antenna element is fed, while the other one is terminated. The measurements agree well with the simulation, which show an acceptable agreement with simulations. It was observed that

the radiation pattern in the xoz-plane is almost omnidirectional in Fig. 7. In the yoz-plane, the radiation patterns are tended to be quasi-directional ones which is similar to the conventional monopole antenna. But the antenna pattern gradually deteriorates with the frequency increasing, and there are some distortions in the high frequency, which are tolerable changes at 10 GHz and 12 GHz shown in Figs. 7 (b) and (c). The reason may be that the added decoupling structure gives a little effects on the direction of the electric field, resulting in the antenna radiation performance to be affected.

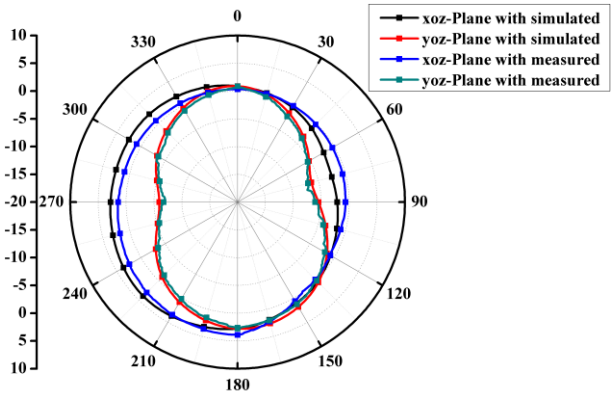


(a) 8 GHz

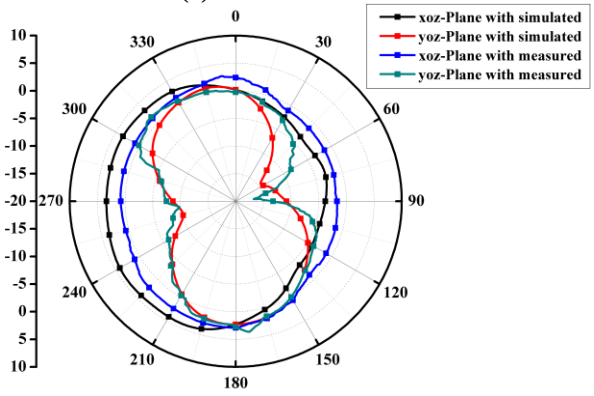


(b) 10 GHz

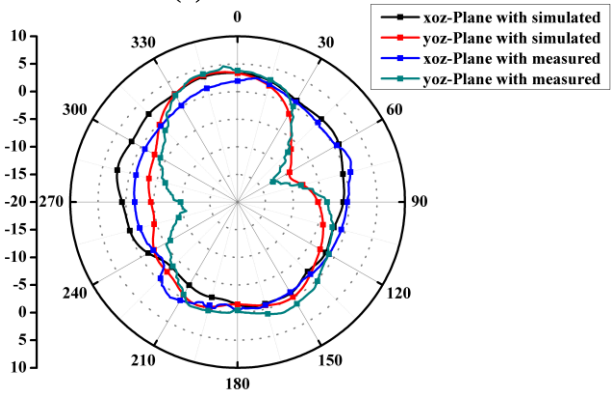


(c) 12 GHz

Fig. 7. The simulated and measured radiation patterns.

In Fig. 8, the gain of the proposed MIMO antenna with wheel-like meta-material structure ranges from 2.67 dBi to 4.62 dBi over the X-band, and the variation in the gain values is found to be less than 2 dBi. Moreover, the maximum gain is 4.62 dBi at 10 GHz, and the minimum gain is 2.67 dBi at 9.4 GHz. The reason may be that the impedance does not match at 9.4 GHz, resulting in part of the energy to be reflected on the feedline and not to be effectively radiated from the antenna.

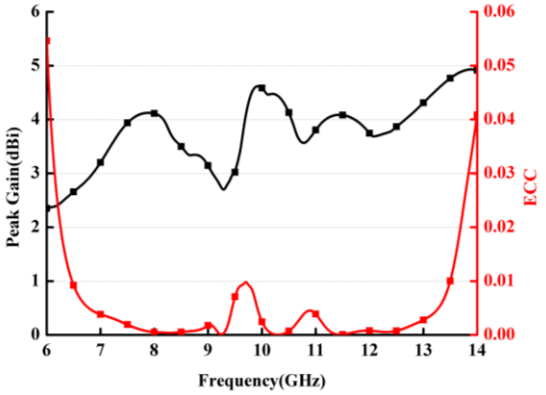


Fig. 8. Gain and ECC of the proposed MIMO antenna array.

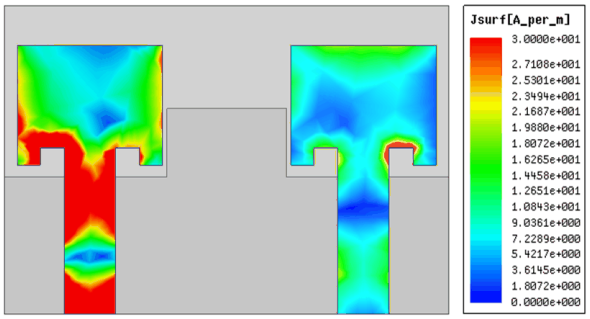


(a) Proposed MIMO antenna array without the decoupling structure

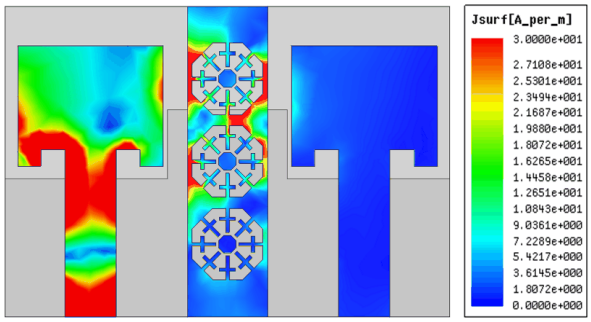


(b) Proposed MIMO antenna array with the decoupling structure

Fig. 9. Surface current distribution on the proposed MIMO antenna array at 11GHz.

The envelope correlation coefficient (ECC) is also important parameter to verify the performance of MIMO antenna. Using the equation in [25], we know that the ECC must be zero in ideal, which is not possible in free space environment. In Fig. 8, the obtained ECC for proposed MIMO antenna array with wheel-like meta-material structure is less than 0.01 within the X-band, which indicates that there is very low correlation between the two ports.

To better demonstrate the effectiveness of the proposed meta-material decoupling structure, the current distribution on the antenna is shown in Fig. 9. In Fig. 9 (a), the current distributions on the proposed MIMO antenna without meta-material decoupling structure is presented, which coupled to the adjacent antenna element when the left antenna is exited. After integrating the proposed meta-material decoupling structure into the middle of the two antenna elements, the surface current on the right antenna is observed to be significantly reduced in Fig. 9 (b). Thus, it is concluded that the proposed wheel-like meta-material decoupling structure can block the surface waves from the left antenna to the right antenna.

## IV. CONCLUSION

A compact wideband MIMO antenna array based on wheel-like meta-material structure with the size of $26 \times 18 \times 1.6$ mm$^3$ has been proposed for X-band communication applications. To suppress mutual coupling between the proposed MIMO antenna elements, a wheel-like meta-material decoupling structure is developed and integrated into the middle of the MIMO antenna array. The MIMO antenna array is designed, simulated, optimized, fabricated and measured, and the results demonstrated that the proposed MIMO antenna array has a wide bandwidth to cover the entire X-band with a fractional bandwidth of 40% and provides a high isolation that is better than 20dB. In addition, the peak gain ranges from 2.67 dBi to 4.62 dBi within the X-band. Moreover, ECC is less than 0.01. Hence, the proposed antenna array is suitable for X-band MIMO radar systems. In the future, the proposed technique can be used for developing the dual-band or dual-polarization low mutual coupling MIMO arrays [26-27], beamforming [28], direction of arrival (DOA) [29-30] using adaptive methods [31-37].

## ACKNOWLEDGMENTS

This paper is supported by the National Key Research and Development Program of China (2016YFE0111100), Key Research and Development Program of Heilongjiang (GX17A016), China Post-doctoral Science Foundation (2017M620918, 2019T120134), the Fundamental Research Funds for the Central Universities (HEUCFG201829, 2072019CFG0801.

## REFERENCES

[1] T. Kaiser, F. Zheng, and E. Dimitrov, "An overview of ultra-wide-band systems with MIMO," *Proceedings of the IEEE*, vol. 97, no. 2, pp. 285-312, 2009.

[2] Y. Li, W. Li, and W. Yu, "A multi-band/UWB MIMO/diversity antenna with an enhance isolation using radial stub loaded resonator," *Applied Computational Electromagnetics Society Journal*, vol. 28, no. 1, pp. 8-20, 2013.

[3] A. Iqbal, O. A. Saraereh, A. W. Ahmad, and S. Bashir, "Mutual coupling reduction using F-shaped stubs in UWB-MIMO antenna," *IEEE Access*, vol. 6, pp. 2755-2759, 2018.

[4] L. Liu, S. Cheung, and T. Yuk, "Compact MIMO antenna for portable devices in UWB applications," *IEEE Transactions on Antennas and Propagation*, vol. 61, no. 8, pp. 4257-4264, 2013.

[5] S. Luo, Y. Li, Y. Xia, G. Yang, L. Sun, and L. Zhao, "Mutual coupling reduction of a dual-band antenna array using dual-frequency metamaterial structure," *Applied Computational Electromagnetics Society Journal*, vol. 34, no. 3, pp. 403-410, 2019.

[6] Y. Kong, Y. Li, and W. Yu, "A minimized MIMO-UWB antenna with high isolation and triple band-notched functions," *Frequenz*, vol. 70, no. 11-12, pp. 463-471, 2016.

[7] S. Luo, Y. Li, Y. Xia, and L. Zhang, "A low mutual coupling antenna array with gain enhancement using metamaterial loading and neutralization line structure," *Applied Computational Electromagnetics Society Journal*, vol. 34, no. 3, pp. 411-418, 2019.

[8] J. Li, X. Zhang, Z. Wang, X. Chen, J. Chen, Y. Li, and A. Zhang, "Dual-band eight-antenna array design for MIMO applications in 5G mobile terminals," *IEEE Access*, vol. 7, pp. 71636-71644, 2019.

[9] T. Jiang, T. Jiao, and Y. Li, "A low mutual coupling MIMO antenna using periodic multi-layered electromagnetic band gap structures," *Applied Computational Electromagnetics Society Journal*, vol. 33, no. 3, 2018.

[10] R. Anitha, V. P. Sarin, P. Mohanan, and K. Vasudevan, "Enhanced isolation with defected ground structure in MIMO antenna," *Electronics Letters*, vol. 50, no. 24, pp. 1784-1786, 2014.

[11] C. Luo, J. Hong, and L. Zhong, "Isolation enhancement of a very compact UWB-MIMO slot antenna with two defected ground structures," *IEEE Antennas and Wireless Propagation Letters*, vol. 14, pp. 1766-1769, 2015.

[12] N. Kishore, A. Prakash, and V. Tripathi, "A multiband microstrip patch antenna with defected ground structure for its applications," *Microwave*

*and Optical Technology Letters*, vol. 58, no. 12, pp. 2814-2818, 2016.

[13] A. Najam, Y. Duroc, and S. Tedjni, "UWB-MIMO antenna with novel stub structure," *Progress In Electromagnetics Research C*, vol. 19, pp. 245-257, 2011.

[14] J. Li, Q. Chu, Z. Li, and X. Xia, "Compact dual band-notched UWB MIMO antenna with high isolation," *IEEE Transactions on Antennas and Propagation*, vol. 61, no. 9, pp. 4759-4766, 2013.

[15] S. Zhang and G. F. Pedersen, "Mutual coupling reduction for UWB MIMO antennas with a wideband neutralization line," *IEEE Antennas and Wireless Propagation Letters*, vol. 15, pp. 166-169, 2016.

[16] H. Huang and J. Wu, "Decoupled dual-antenna with three slots and a connecting line for mobile terminals," *IEEE Transactions on Antennas and Propagation*, vol. 14, pp. 1730-1733, 2015.

[17] Q. Li, A. Feresidis, M. Mavridou, and P. Hall, "Miniaturized double-layer EBG structures for broadband mutual coupling reduction between UWB monopoles," *IEEE Transactions on Antennas and Propagation*, vol. 63, no. 3, pp. 1170-1173, 2015.

[18] T. Jiang, T Jiao, and Y. Li, "Array mutual coupling reduction using L-loading E-shaped electromagnetic band gap structures," *International Journal of Antennas and Propagation*, vol. 2016, pp. 1-9, 2016.

[19] F. Yang, K. Ma, Y. Qian, and T. Itoh, "A uniplanar compact photonic-bandgap (UC-PBG) structure and its applications for microwave circuit," *IEEE Transactions on Microwave Theory and Techniques*, vol. 47, no. 8, pp. 1509-1514, 1999.

[20] K. Niraj and K. Usha, "MIMO antenna H-plane isolation enhancement using UC-EBG structure and metal line strip for WLAN applications," *Radioengineering*, vol. 28, no. 2, pp. 399-406, 2019.

[21] Y. Ranga, L. Matekovits, K. P. Esselle, and A. R. Weily, "Multioctave frequency selective surface reflector for ultrawideband antennas," *IEEE Antennas and Wireless Propagation Letters*, vol. 10, pp. 219-222, 2011.

[22] X. Zhu, X. Yang, Q. Song, and B. Lui, "Compact UWB-MIMO antenna with metamaterial FSS decoupling structure," *EURASIP Journal on Wireless Communications and Networking*, 2017.

[23] A. Mansoor and R. Amiri, "Mutual coupling reduction of closely spaced MIMO antenna using frequency selective surface based on meta-materials," *Applied Computational Electromagnetics Society Journal*, vol. 32, no. 12, pp. 1064-1068, 2017.

[24] X. Chen, T. M. Grzegorczyk, B. Wu, J. Pacheco, and J. Kong, "Robust method to retrieve the constitutive effective parameters of metamaterials," *Physical Review E*, vol. 70, no. 1, 2004.

[25] R. Tian, B. K. Lau, and Z. Ying, "Multiplexing efficiency of MIMO antennas," *IEEE Antennas and Wireless Propagation Letters*, vol. 10, pp. 183-186, 2011.

[26] F. Liu, J. Guo, L. Zhao, G.L. Huang, Y. Li, and Y. Yin, "Dual-band metasurface-based decoupling method for two closely packed dual-band antennas," *IEEE Transactions on Antennas and Propagation*, 10.1109/TAP.2019.2940316.

[27] J. Guo, F. Liu, L. Zhao, Y. Yin, G. L. Huang, and Y. Li, "Meta-surface antenna array decoupling designs for two linear polarized antennas coupled in H-plane and E-plane," *IEEE Access*, vol. 7, pp. 100442-100452, 2019.

[28] W. Shi, Y. Li, L. Zhao, and X. Liu, "Controllable sparse antenna array for adaptive beamforming," *IEEE Access*, vol. 7, pp. 6412-6423, 2019.

[29] X. Zhang, T. Jiang, Y. Li, and X. Liu, "An off-grid DOA estimation method using proximal splitting and successive nonconvex sparsity approximation," *IEEE Access*, vol. 7, pp. 66764-66773, 2019.

[30] X. Zhang, T. Jiang, Y. Li, and Y. Zakharov, "A novel block sparse reconstruction method for DOA estimation with unknown mutual coupling," *IEEE Communications Letters*, vol. 23, no. 10, pp. 1845-1848, 2019.

[31] W. Shi, Y. Li, and Y. Wang, "Noise-free maximum correntropy criterion algorithm in non-gaussian environment," *IEEE Transactions on Circuits and Systems II: Express Briefs*, 10.1109/TCSII.2019.2914511.

[32] Y. Li, Z. Jiang, W. Shi, X. Han, and B. Chen, "Blocked maximum correntropy criterion algorithm for cluster-sparse system identifications," *IEEE Transactions on Circuits and Systems II: Express Briefs*, 10.1109/TCSII.2019.2891654.

[33] Y. Li, Z. Jiang, O. M. O. Osman, X. Han, and J. Yin, "Mixed norm vonstrained sparse APA algorithm for satellite and network echo channel estimation," *IEEE Access*, vol. 6, pp. 65901-65908, 2018.

[34] Y. Li, Y. Wang, and T. Jiang, "Norm-adaption penalized least mean square/fourth algorithm for sparse channel estimation," *Signal Processing*, vol. 28, pp. 243-251, 2016.

[35] Y. Li, Y. Wang, and T. Jiang, "Sparse-aware set-membership NLMS algorithms and their application for sparse channel estimation and echo cancelation," *AEU-International Journal of Electronics and Communications*, vol. 70, no. 7, pp. 895-902, 2016.

[36] Y. Li, Z. Jiang, Z. Jin, X. Han, and J. Yin, "Cluster-sparse proportionate NLMS algorithm with the hybrid norm constraint," *IEEE Access*, vol. 6, pp. 47794-47803, 2018.
[37] Q. Wu, Y. Li, Y. Zakharov, W. Xue, and W. Shi, "A kernel affine projection-like algorithm in reproducing kernel hilbert space," *IEEE Transactions on Circuits and Systems II: Express Briefs*, 10.1109/TCSII.2019.2947317.